Diabetes, Metabolic Syndrome and Obesity

Dovepress
Taylor & Francis Group

Open Access Full Text Article

ORIGINAL RESEARCH

Comparison of MR Spectroscopy, 2-Point Dixon, and Multi-Echo T2* Sequences in Assessing Hepatic Fat Fraction Across a Diverse Range of Body Mass Index (BMI) and Waist Circumference Ratio (WCR) Values

Beata Brzeska[1], Agnieszka Sabisz[1], Oliwia Kozak[2], Edyta Szurowska[1], Joanna Pieńkowska[1]

[1]II Department of Radiology, Faculty of Health Studies, Medical University of Gdansk, Gdansk, Poland; [2]I Department of Radiology, Faculty of Medicine, Medical University of Gdansk, Gdansk, Poland

Correspondence: Beata Brzeska, Email beabrzes@gumed.edu.pl

Objective: The study aimed to compare and evaluate the accuracy of three magnetic resonance imaging (MRI) sequences—MR liver spectroscopy, 2-point Dixon, and multi-echo T2*—in assessing hepatic fat fraction in patients with various body mass indexes (BMIs).
Methods: 167 participants were recruited, including 110 healthy subjects with diverse BMIs and 57 bariatric surgery candidates. The MRI protocol involved three sequences: multi-echo single voxel STEAM 1H spectroscopy, 2-point mDixon, and multi-echo T2* sequence. Hepatic fat fraction was measured using these sequences and analyzed statistically to determine correlations and agreement between the methods.
Results: A strong positive correlation was observed between BMI and waist circumference ratio (WCR) ($r_s(165) = 0.910$, $p<0.001$). MRS obtained hepatic fat fraction numerical values in 13.33% of the normal BMI group, 48.48% of the overweight group, and 72.97% of the obese group. Strong correlations were found between all methods, with significant agreement, particularly between MRS and multi-echo T2*.
Conclusion: Robust correlations were observed between MR spectroscopy, 2-point Dixon, and multi-echo T2* methods for liver fat fraction measurement, especially in patients with higher BMI and WCR. These findings highlight the importance of BMI and WCR in interpreting fat fraction measurements, as method performance can vary across body composition profiles.
Keywords: magnetic resonance imaging, 1HNMR liver spectroscopy, hepatic steatosis

Introduction

Hepatic steatosis, characterized by fat accumulation in liver cells, is a prevalent health concern associated with various metabolic disorders. The occurrence of hepatic steatosis is closely tied to the increasing rates of obesity and metabolic syndrome across diverse populations worldwide.

Obesity, characterized by an excess accumulation of body fat, is a primary risk factor for the development and progression of hepatic steatosis. It is typically determined by the body mass index (BMI), calculated by dividing an individual's weight in kilograms by the square of their height in meters. A BMI of 30 or higher is commonly used to define obesity. Obesity is a significant public health concern worldwide, associated with an increased risk of various chronic conditions such as cardiovascular diseases, diabetes, and certain cancers. According to WHO, in 2016, 39% of adults were overweight and 13% were obese, and between 1975 and 2016, the worldwide prevalence of obesity nearly tripled.[1,2]

Metabolic syndrome is a well-established precursor to hepatic steatosis. The presence of three out of five abnormal components qualifies a patient for metabolic syndrome: central obesity, high blood pressure, elevated fasting plasma

Received: 2 June 2024
Accepted: 21 January 2025
Published: 26 February 2025

glucose level, high triglyceride level, and decreased high-density lipoprotein cholesterol level. Individuals with metabolic syndrome often exhibit insulin resistance, contributing to glucose and lipid metabolism dysregulation. Lifestyle factors such as sedentary behaviour, poor diet, and genetic predisposition play vital roles in the development of metabolic syndrome, making it a critical public health concern.[3–8]

BMI is a commonly used metric for assessing body fat based on an individual's weight in relation to their height. While BMI does not directly measure body fat percentage, it is a convenient and widely accepted indicator of body fat levels in population studies. In hepatic steatosis studies, BMI plays a crucial role. It provides a quick and standardized way to categorize individuals into different weight classes, such as underweight, normal weight, overweight, and obese. Elevated BMI is often associated with an increased risk of hepatic steatosis.[9] However, it may not capture variations in body composition, and additional assessments may be needed for a more comprehensive understanding of an individual's health status.[10]

As societies transition in dietary habits and experience sedentary lifestyles, the global burden of hepatic steatosis is expected to rise further. Not only does this prevalence pose a substantial public health challenge but it also contributes to the overall burden of liver-related morbidity and mortality.[11]

Accurate assessment of hepatic fat content is crucial for understanding disease progression and guiding therapeutic interventions.[12] Among various diagnostic tools, Proton Magnetic Resonance Spectroscopy (1H MRS) stands out for its accuracy in assessing hepatic steatosis, as evidenced by its strong correlation with biopsy results.[13–16] However, precision in both the acquisition and post-processing stages is critical, requiring skilled operators to ensure accurate results. Variability in the positioning of the spectroscopy voxel and susceptibility to motion artifacts can introduce errors in the data. Additionally, factors such as the presence of iron in the liver or the coexistence of other liver pathologies can complicate the interpretation of spectroscopic signals, potentially leading to inaccuracies.[17]

Another MRI sequence commonly used for hepatic fat assessment is the two-point Dixon method. Noteworthy for its ease of acquisition and reduced post-processing demands compared to 1H MRS, the two-point Dixon method is widely available, can be acquired in one breath-hold, and its diagnostic performance remains robust for most nondemanding cases. However, its reliance on only two echo times may lead to inaccuracies, especially in tissues with varying fat composition or elevated iron content, as it does not fully account for T2* decay.[18,19]

It is also possible to use a vendor-neutral alternative such as MRQuantif, the quantification software developed by Rennes University Hospital. MRQuantif enables consistent fat fraction and iron quantification across different MRI systems, enhancing accessibility and potentially broadening clinical application without requiring specific calibration for each MRI vendor. The software uses a standardized multi-echo 2D sequence for steatosis and iron overload quantification. The multi-echo imaging technique enhances the ability to correct for T2 relaxation effects, offering superior accuracy in hepatic fat fraction quantification compared to the two-point Dixon method, especially in patients with varying hepatic composition.[20] A recent study showed that the fat fraction provided by this software correlates well with the values obtained by histomorphometry.[21] However, the multi-echo sequence used with this software is a single-slice technique, and thus, variability in slice positioning can introduce errors in fat quantification.

The challenges in different magnetic resonance (MR) hepatic fat assessment methods can be influenced by patients' diverse body mass index (BMI) ranges. One significant challenge is achieving consistent image quality across varying BMIs. Increased adiposity in patients with higher BMI can lead to signal attenuation, particularly in liver regions farther from the MRI coil. This signal loss reduces the signal-to-noise ratio (SNR) and can impair image resolution, which may contribute to inaccuracies in fat quantification.[22] However, these challenges - related to RF penetration, tissue composition, and signal attenuation - are common across all MRI sequences used for hepatic fat assessment. Additionally, the accuracy of fat quantification may be affected by variations in tissue composition related to BMI, leading to potential biases in the assessment.[23] Patient positioning and motion artifacts, particularly challenging in individuals with higher BMIs, can also compromise the precision of MR fat quantification. It is crucial to address these BMI-related challenges systematically to ensure the reliability and applicability of MR hepatic fat assessment across a broad spectrum of patients.

This study aimed to compare and evaluate the efficiency of MR liver spectroscopy, 2-point Dixon, and multi-echo T2* sequences in patients with various BMIs.

Materials and Methods

Participants

The study was conducted in accordance with the Declaration of Helsinki. The protocol was approved by the Independent Bioethics Commission for Research at the Medical University of Gdansk, Poland. Before undergoing abdominal magnetic resonance imaging, all participants were informed about the procedures, risks, and expected outcomes and gave their written informed consent for participation.

110 healthy subjects with various BMIs were recruited for the abdominal MRI. Additionally, to expand the group and include cases with higher BMI, 57 patients from the Department of General, Endocrine and Transplant Surgery, University Clinical Centre in Gdansk, who were referred for bariatric surgery, were also enrolled in the study. All bariatric patients had their abdominal circumference measured before being referred for imaging to ensure that the bore diameter of the MR scanner was sufficient. A medical interview was collected from all participants to rule out any health problems (other than obesity), excessive alcohol consumption, or any existing metal implants and pacemakers. The selection of subjects was not planned statistically. Recruitment for this study and all the MRI examinations were conducted between 1 July 2018 and 31 August 2019 at the Department of Radiology, University Clinical Centre in Gdansk, Poland. Prior to data analysis, liver iron concentration (LIC) was calculated for all participants using MRQuantif, as described in the Data analysis section. One participant with a liver iron concentration above the normal range was excluded from the study to avoid potential interference with fat fraction measurements. Ultimately, the study involved 167 patients (114 women, mean age 40.18±11.42 years, range 19–71, and 53 men, mean 39.45±11.59 years, range 18–65).

For all participants, Body Mass Index (BMI) was computed by dividing weight in kilograms by the square of height in meters, with recognized BMI ranges applied: underweight (<18.5 kg/m²), normal weight (18.5–24.9), overweight (25–29.9), and obese (≥30 kg/m²).

Waist circumference was measured horizontally midway between the lower rib margin and the iliac crest. Central obesity was determined using ethnicity-specific waist circumference values in Europe, which is ≥80 cm for women and ≥94 cm for men. Due to the gender-dependent variations in reference values, a universally applicable metric called Waist Circumference Ratio (WCR) has been applied as previously.[24,25] The WCR [%] is calculated as the ratio of the patient's waist circumference to the respective reference value (80 cm for women and 94 cm for men). For women, a WCR of 100% corresponds to the limit value of 80 cm, with values below 100% indicating a normal waist circumference (<80 cm) and those exceeding 100% indicative of central obesity. Similarly, for men, a WCR of 100% corresponds to the limit value of 94 cm, with values below 100% indicating a normal waist circumference (<94 cm) and those exceeding 100% indicative of central obesity. Detailed data on participants' BMI and WCR are provided in Table 1.

Magnetic Resonance Imaging

All MRI examinations were performed on a 3.0 T scanner (Achieva TX, Philips, Best, The Netherlands) using the 16-channel Sense XL Torso Coil. The study protocol included three sequences to evaluate hepatic fat fraction (FF): multi-echo single voxel STEAM 1H spectroscopy, 2-point mDixon, and multi-echo T2* sequence.

Planning for 1H single-voxel MRS was performed on transversal T2-weighted turbo spin-echo, coronal T2-weighted SPAIR, and sagittal BTFE images. The STEAM technique was used for MRS to enable short TE. 5 TEs (12, 24, 36, 48, and 72ms) were acquired during separate one breath-hold acquisitions without water suppression. 20x20x30 mm voxels were placed in the homogeneous liver parenchyma, avoiding enlarged bile ducts and large vessels. Other acquisition parameters were TR 2000ms, 8 averages, and 1024 points.

2-point mDixon parameters were as follows: TR 3.6ms, TE 1.31 and 2.3ms, slice thickness 5 mm, FoV 385×385 mm, matrix size 320 x 190, transversal orientation. Acquisition time below 20s allowed for one breath-hold acquisition. Water-only and fat-only images were also created.

A single gradient echo T2* sequence, designed for the Philips Achieva scanner and compatible with the MRQuantif software, was downloaded directly from the University of Rennes website.[26] Only the system body coil was selected for acquisition as recommended. The sequence included 10 echoes with TEs multiple of 1.2ms starting from 1.2ms. Two or three single-slice acquisitions were performed for each patient to cover the same liver region selected for MRS.

Table 1 Characteristics of the BMI Groups in the Study

		BMI group		
		18.5–24.9 [$\frac{kg}{m^2}$] (normal)	**25–29.9 [$\frac{kg}{m^2}$] (overweight)**	**≥30 [$\frac{kg}{m^2}$] (obese)**
Number of patients		60	33	74
Gender (F-female, M-male)		40 F, 20 M	15 F, 18 M	59 F, 15 M
Age	Range	18–65	26–71	21–59
	Mean ± SD	38.22 ± 12.24	42.58 ± 12.94	40.18 ± 9.88
	Median	34.50	42.00	38.00
	Q1, Q3	28.00, 45.25	31.00, 52.00	32.25, 49.00
BMI [$\frac{kg}{m^2}$]	Range	18.59–24.97	25.00–29.74	30.07–47.83
	Mean ± SD	22.07 ± 1.78	26.96 ± 1.45	37.45 ± 4.07
	Median	22.41	26.59	37.53
	Q1, Q3	20.71, 23.24	25.59, 28.16	35.22, 39.13
WCR [%]	Range	76.77–119.38	91.05–130.34	109.10–160.00
	Mean ± SD	96.57 ± 7.89	110.09 ± 9.60	137.71 ± 11.71
	Median	96.20	111.23	138.75
	Q1, Q3	90.71, 100.81	102.29, 117.49	129.04, 146.10

Data Analysis

The acquired MRS spectra were analyzed in the java-based MR user interface (jMRUI) spectroscopic analysis package using the Advanced Magnetic Resonance (AMARES) fitting algorithm. For all TEs amplitudes of water (4.7 ppm) and fat (1.3 ppm) peaks were measured (Figure 1). Peak integrals were quantified by fitting to a Gaussian line shape. T2 relaxation times and theoretic peak areas for 0ms TE (A_0) of water and fat were determined from their peak amplitudes at each TE using an exponential least-squares fitting algorithm. To correct for T2 effects, A_0 of fat and water were used to calculate the hepatic percentage fat content:[27]

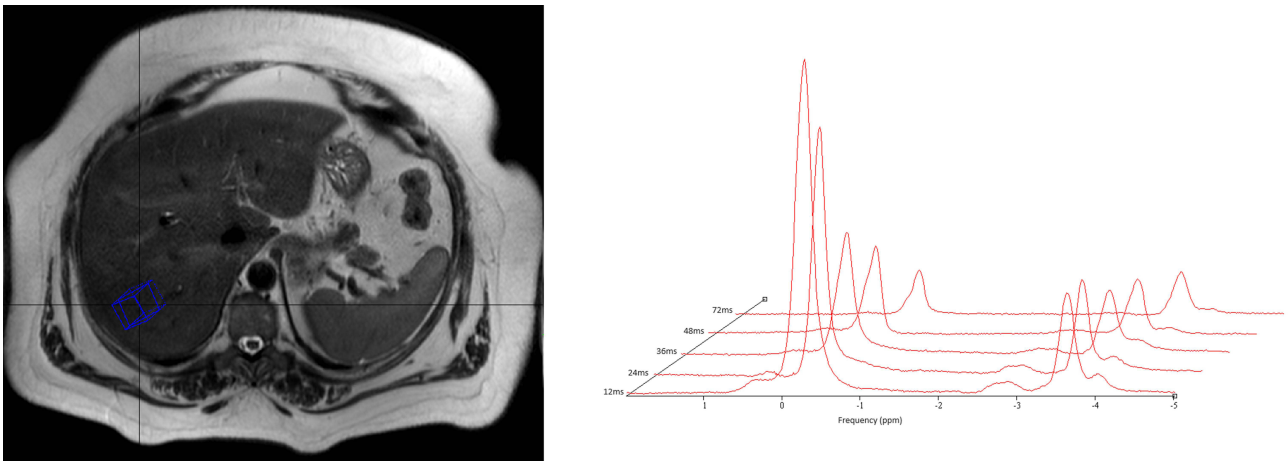

Figure 1 Left: Positioning of MRS voxel on T2 turbo spin echo transversal MR image. Right: ^{1}HNMR spectra with 5 TE to calculate T2 relaxation times of water and fat.

$$F_{MRS} = 100\frac{A_{0\,fat}}{A_{0\,fat} + A_{0\,water}}[\%]$$

Three regions of interest (ROIs) were placed on the water- and fat-only images to assess the liver fat content from Dixon images. ROIs were as large as possible, avoiding large vessels and bile ducts. Mean signal intensity for water-only and fat-only images was used to calculate the liver fat fraction by dividing the fat signal intensity by the sum of the fat and water signals.

The multi-echo T2* sequence data were analyzed in MRQuantif software by placing three ROIs of 5 cm² in the liver, in the same locations as in the Dixon analysis. Two smaller ROIs were placed on the paraspinal muscles as the reference for the iron quantification, and one additional ROI was placed outside of the body to measure the background noise. The software propagates all the ROIs to the exact location to all different TE images and generates an automatic report about iron overload and fat content in selected organs.

Statistical Analysis

The normality assumption of the data was assessed by the Kolmogorov-Smirnov and Shapiro–Wilk tests, depending on the size of the variable. Linear regression was performed to present a graphic correlation between BMI and WCR. Spearman's rank correlation was calculated to estimate the strength of the relation between BMI, WCR, and different steatosis assessment methods. The agreement between these methods was evaluated with a Bland-Altman plot. The level of significance was set at $p<0.05$. All statistical analyses were performed using Statistical Package for Social Sciences (SPSS) software, version 29 (IBM, New York, US).

Results

There was a strong, positive correlation between BMI and waist circumference ratio (WCR) ($r_s(165) = 0.910$, $p<0.001$) in the study population. Linear regression graph (Figure 2) showed that when BMI increased by one unit, WCR increased by 2.57% (R=0.92).

Of 167 patients, only 78 patients (47%) had a measurable fat peak on at least 2 TEs from the acquired MRS spectra, which made it possible to calculate the hepatic fat fraction with the T2 correction. For 89 patients, the fat peak was visible only on 72ms TE or was not visible in any spectra. In the group with a normal BMI, hepatic FF from MRS was obtained in 13.33% of the group; in overweight patients, it was 48.48%, and in obese patients, it was 72.97%. Similarly, for patients with WCR below 100%, the FF from MRS was obtained in 10% of the patients, while it was 47.73% in patients with WCR between 100 and 120%, 59.46 in patients with 120–140% WCR, and 83.33% in the group of WCR above 140%.
Detailed information is provided in Table 2.

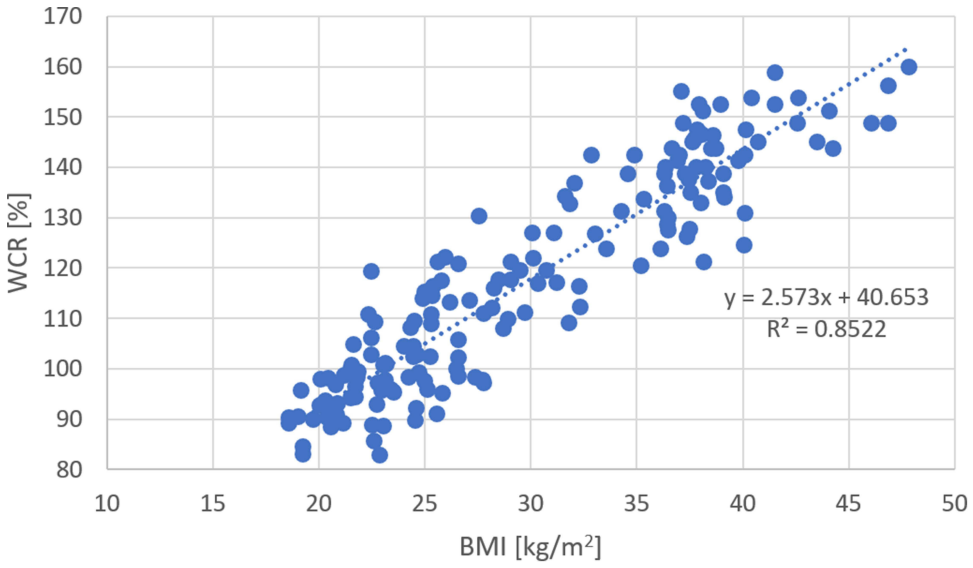

Figure 2 Linear correlation between Waist Circumference Ratio and BMI.

https://doi.org/10.2147/DMSO.S481062

Table 2 MR Spectroscopy Performance in Different BMI and WCR Groups

Group of Patients		Number of Patients	Number of Patients with Sufficient Information to Obtain FF from MRS	% of the Group
BMI	Normal	60	8	13.33
	Overweight	33	16	48.48
	Obese	74	54	72.97
WCR	<100%	50	5	10.00
	100%-120%	44	21	47.73
	120%-140%	37	22	59.46
	>140%	36	30	83.33

For 89 patients with no outcome from MRS, the mean fat fraction in other methods was 1.22±0.93% for multi-echo T2* and 6.37±1.88% for the 2-point Dixon method.

To examine differences between patients with and without measurable MRS outcomes, Mann–Whitney *U*-test was conducted on key variables, including Dixon FF, T2* FF, BMI, and WCR. The results indicated statistically significant differences ($p < 0.001$) between the two groups across all variables.

Further analyses were performed for 78 patients for whom all fat fraction measurements, including MRS, provided a numerical value. Descriptive statistics on MRS, multi-echo T2*and 2-point Dixon fat fractions in various BMI and WCR groups are presented in Table 3. Scatter plots showing the relationship between BMI and WCR and hepatic fat fraction for each imaging method (MRS, 2-point Dixon, and multi-echo T2*) are presented in Figure 3a and b.

Table 3 Descriptive Statistics on MRS, Multi-Echo T2*, and 2-Point Dixon Fat Fractions in Various BMI (a) and WCR (b) Groups

a)				
		BMI [$\frac{kg}{m^2}$]		
		18.5–24.9 (normal)	**25–29.9 (overweight)**	**≥30 (obese)**
MRS FF [%]	Range	0.27–1.39	0.27–15.57	0.33–32.89
	Mean ± SD	0.91 ± 0.41	4.04 ± 4.59	9.94 ± 7.69
	Median	0.93	1.99	8.75
	Q1, Q3	0.70, 1.25	0.84, 6.58	3.77, 14.61
Multi-echo T2* FF [%]	Range	1.00–4.00	0.00–17.00	1.00–28.00
	Mean ± SD	2.13 ± 1.13	4.88 ± 4.24	10.30 ± 6.68
	Median	2.00	3.50	9.00
	Q1, Q3	1.00, 3.00	2.00, 6.25	5.00, 15.75
2-point Dixon FF [%]	Range	5.38–10.05	5.51–30.72	7.33–46.67
	Mean ± sd	7.22 ± 1.39	13.16 ± 6.77	24.13 ± 10.92
	Median	7.07	12.36	22.74
	Q1, Q3	6.48, 7.60	8.05, 15.30	15.67, 32.75

(*Continued*)

Table 3 (Continued).

b)					
		WCR [%]			
		<100	100–120	120–140	≥140
MRS FF [%]	Range	0.46–1.32	0.27–15.57	0.27–18.89	0.33–32.89
	Mean ± SD	1.00 ± 0.35	5.38 ± 5.14	7.02 ± 5.77	11.22 ± 9.02
	Median	1.15	3.21	6.26	9.33
	Q1, Q3	0.87, 1.23	0.88, 8.72	2.45, 9.12	3.99, 17.44
Multi-echo T2* FF [%]	Range	1.00–3.00	0.00–17.00	2.00–18.00	1.00–28.00
	Mean ± SD	2.20 ± 0.84	5.81 ± 4.66	7.86 ± 5.18	11.50 ± 7.70
	Median	2.00	5.00	6.00	9.00
	Q1, Q3	2.00, 3.00	2.00, 8.00	3.25, 10.00	6.00, 18.00
2-point Dixon FF [%]	Range	5.38–10.05	6.53–30.72	5.51–36.12	7.33–46.67
	Mean ± SD	7.36 ± 1.87	15.45 ± 8.14	19.04 ± 9.71	26.38 ± 12.05
	Median	6.61	14.06	18.17	23.33
	Q1, Q3	6.34, 8.45	7.76, 20.96	11.52, 24.89	16.42, 36.33

Spearman's rank correlation between different steatosis methods was calculated, revealing a strong, significant correlation between all methods ($r_s(76) = 0.904$ for multi-echo T2* and Dixon (Figure 4), 0.936 for multi-echo T2* and MRS (Figure 5), and 0.937 for MRS and Dixon (Figure 6), $p<0.001$). Agreement between methods was checked with Bland-Altman plots. One-sample *T*-test showed a p-value < 0.001 for the difference between Dixon FF and MRS FF and between Dixon FF and multi-echo T2* FF. The P-value for the MRS FF and multi-echo T2* FF difference was not statistically significant (p=0.06), so the Bland-Altman plot was constructed to compare these methods (Figure 7). Mean difference of hepatic fat fraction between MR spectroscopy and multi-echo T2* was −0.54 ± 2.5% (95% CI −5.44%, 4.36%).

The relationships among the three MR methods for obtaining fat fraction in different BMI and Waist Circumference Ratio groups were investigated using Spearman correlation analysis. In patients with normal BMI, the group was restricted to only 8 patients, and in patients with a WCR below 100%, the group size was 5. As a result of these small sample sizes, Spearman correlation analysis in these groups was omitted due to inadequate statistical power and the unreliability in estimating correlations. Correlations between MRS, multi-echo T2*and two-point Dixon fat fractions in various BMI and WCR groups are presented in Table 4.

Discussion

The present study aimed to compare and evaluate the efficiency of three magnetic resonance imaging sequences – MR liver spectroscopy, 2-point Dixon, and multi-echo T2* - in assessing hepatic fat fraction across a diverse range of Body Mass Index (BMI) and Waist Circumference Ratio (WCR) values. The study included 167 participants, combining healthy subjects and bariatric surgery candidates, which allowed for a broad representation of BMI values.

The observed strong, positive correlation between BMI and WCR in the study population ($r_s(165) = 0.910$, $p<0.001$) reaffirms the well-established association between central obesity and elevated BMI.[7] The linear regression analysis demonstrated that for every one-unit increase in BMI, there was a corresponding 2.57% increase in WCR, emphasizing the interdependence of these anthropometric measures.

https://doi.org/10.2147/DMSO.S481062

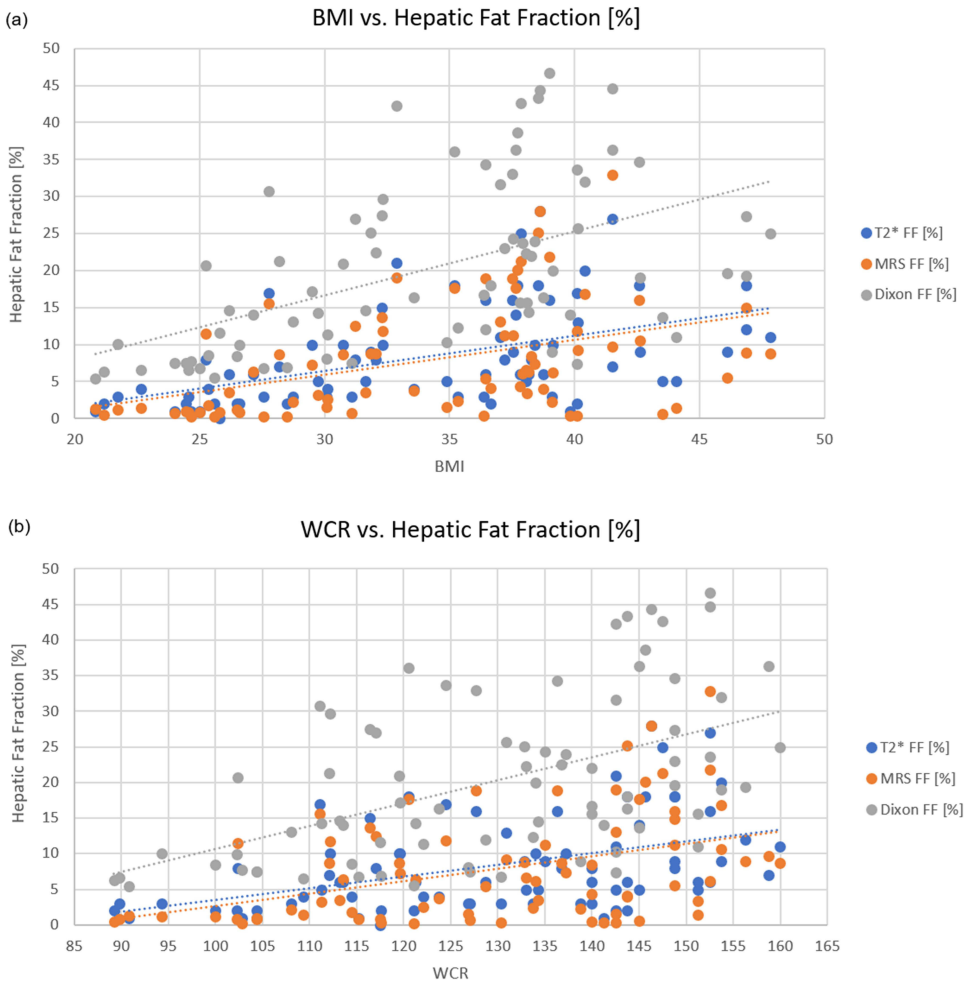

Figure 3 (**a**) Scatter plot of BMI vs hepatic fat fraction (**b**) Scatter plot of WCR vs hepatic fat fraction.

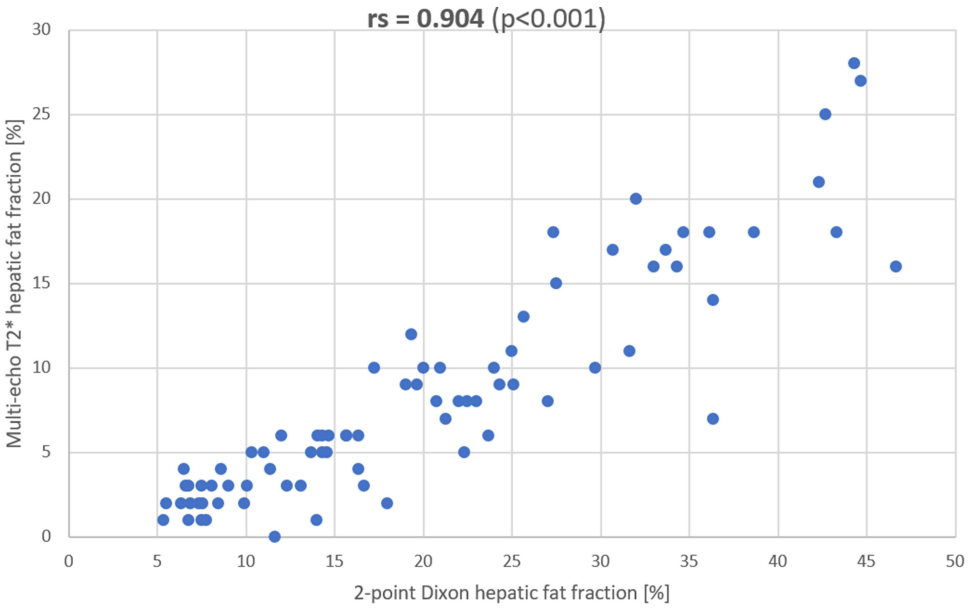

Figure 4 Correlation between 2-point Dixon and multi-echo T2* hepatic fat fraction.

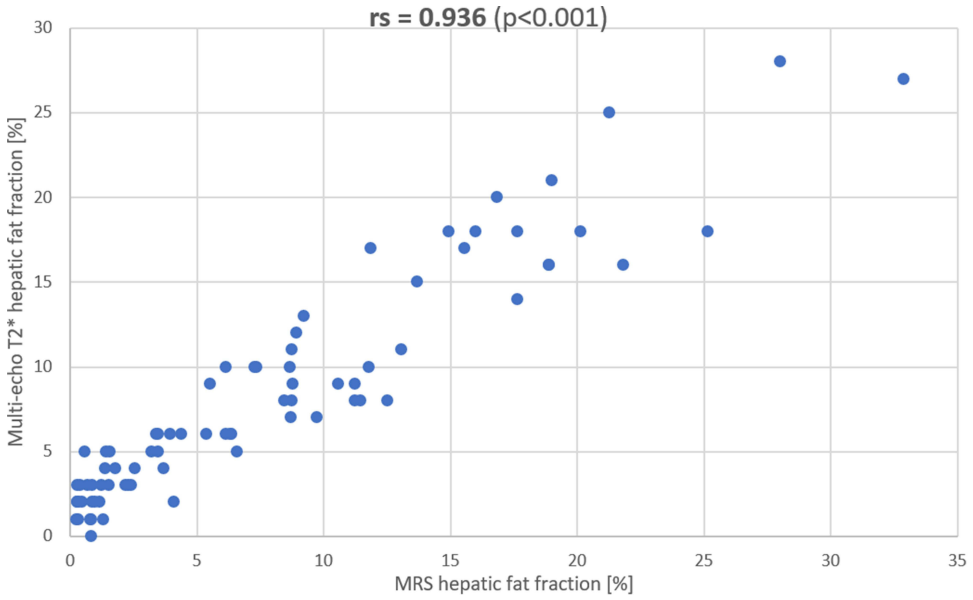

Figure 5 Correlation between MRS and multi-echo T2* hepatic fat fraction.

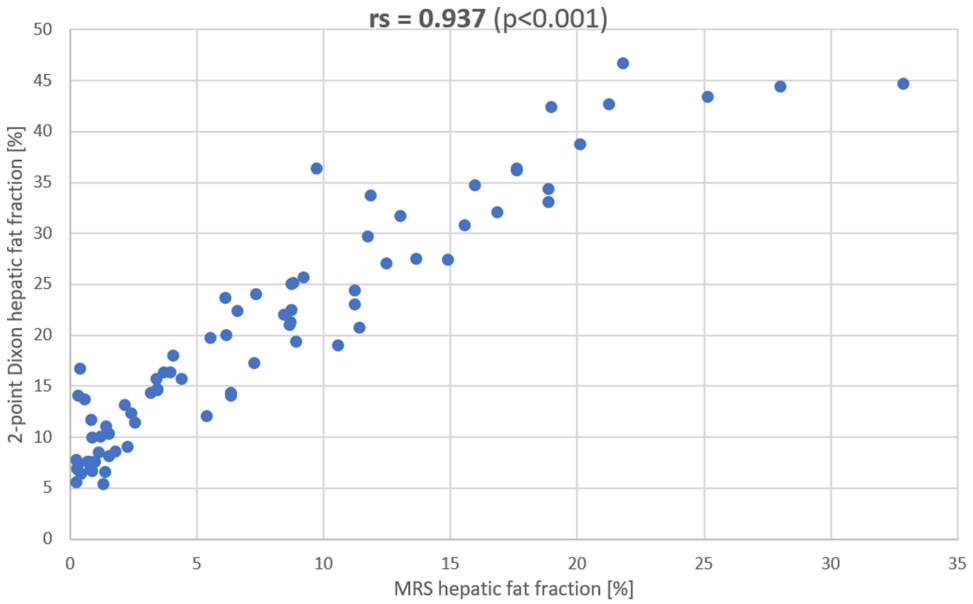

Figure 6 Correlation between MRS and 2-point Dixon hepatic fat fraction.

Notably, the study reported differences in the ability of each imaging method to provide numerical values of hepatic fat fraction. While MRS often did not yield a quantitative FF in some cases, the 2-point Dixon method and multi-echo T2* sequences more consistently produced numerical fat fraction values across different BMI categories. In the group of patients with a normal BMI, MRS provided measurable fat fraction values in only 13.33% of cases. Similarly, for patients with WCR below 100%, MRS produced a quantitative FF value in only 10% of cases. This absence of a measurable value, particularly in patients with low BMI and WCR, may itself be informative, potentially indicating minimal hepatic fat content, possibly near 0%.

To explore the potential differences between patients with and without measurable MRS outcomes, the Mann–Whitney *U*-test was conducted for key variables, including Dixon FF, T2* FF, BMI, and WCR. The results showed

https://doi.org/10.2147/DMSO.S481062

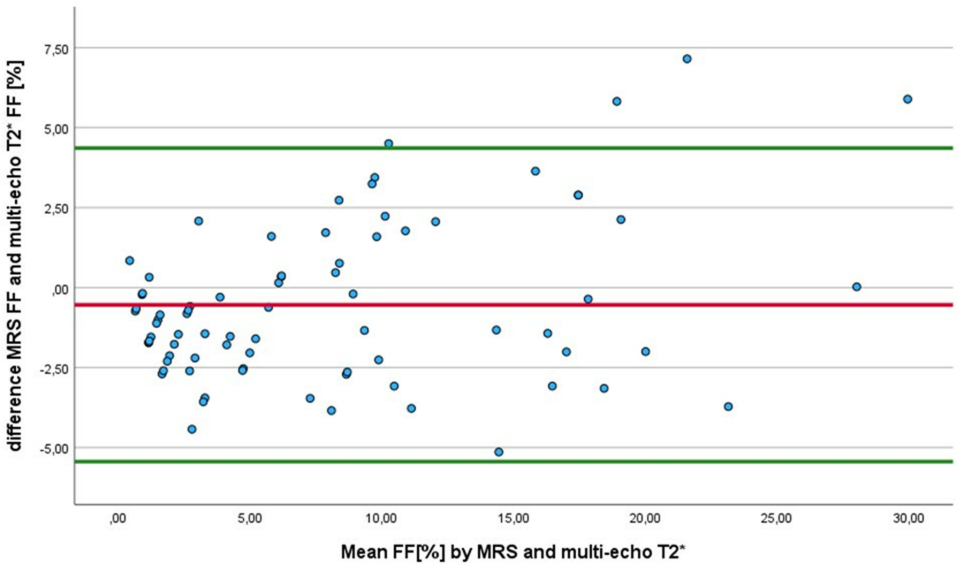

Figure 7 Bland-Altman analysis exploring the mean difference in fat fraction between MRS and multi-echo T2* sequence.

statistically significant differences ($p < 0.001$) across all variables between the groups. This finding supports the interpretation that measurable characteristics differ between patients with and without MRS outcomes, indicating that the absence of measurable MRS values corresponds to minimal hepatic fat content in most cases.

Table 4 Spearman Correlation Factors Between FF Methods in Various BMI and WCR Groups

		r_s	MRS FF	Multi-echo T2* FF	Dixon FF
BMI	Overweight	MRS FF	1.000	0.886*	0.950*
		Multi-echo T2* FF	0.886*	1.000	0.835*
		Dixon FF	0.950*	0.835*	1.000
	Obese	MRS FF	1.000	0.927*	0.943*
		Multi-echo T2* FF	0.927*	1.000	0.884*
		Dixon FF	0.943*	0.884*	1.000
WCR	100–119.9%	MRS FF	1.000	0.942*	0.918*
		Multi-echo T2* FF	0.942*	1.000	0.859*
		Dixon FF	0.918*	0.859*	1.000
	120–139.9%	MRS FF	1.000	0.942*	0.971*
		Multi-echo T2* FF	0.942*	1.000	0.937*
		Dixon FF	0.971*	0.937*	1.000
	>140%	MRS FF	1.000	0.939*	0.949*
		Multi-echo T2* FF	0.939*	1.000	0.874*
		Dixon FF	0.949*	0.874*	1.000

Note: *p<0.001 (2-tailed).

Although a lack of measurable MRS outcomes may indicate minimal hepatic fat, assigning a uniform 0% fat fraction is not always accurate. The analysis showed that the two other methods (2-point Dixon and multi-echo T2) provided different numerical values for hepatic fat in patients without measurable MRS outcomes, indicating that these cases may not uniformly represent 0% fat content. The mean fat fraction in patients with no outcome from MRS was 1.22±0.93% for multi-echo T2 and 6.37±1.88% for the 2-point Dixon method. Additionally, some cases without measurable MRS values may have been impacted by practical challenges during acquisition, such as inconsistent breath-holding between MRS and imaging sequences, which can alter the voxel position relative to the liver. This may lead to non-quantifiable results in MRS even when hepatic fat is present. For these reasons, these cases were excluded from the correlational analysis to avoid introducing assumptions that might bias the results.

Nevertheless, the limited number of cases with measurable MRS values in this study's low BMI and WCR groups posed challenges to making meaningful comparisons with other methods. Thus, in patients with low BMI, if the objective is simply to exclude hepatic steatosis, MRS may be sufficient, as a lack of measurable values likely reflects minimal hepatic fat. However, if precise quantitative tracking is required, such as for follow-up assessments, the 2-point Dixon or multi-echo T2 sequences may be preferred for their consistency in providing numeric fat fraction values.

For 78 patients for whom all fat fraction measurements, including MRS, provided numerical values, correlation analysis demonstrated strong, significant correlations between all methods (r_s>0.9, p<0.001). It revealed strong inter-method correlations in assessing steatosis, supporting the interchangeability of these techniques in clinical settings. Despite strong correlations, we showed a statistically significant difference between mean fat fraction results between two-point Dixon and MRS and between 2-point Dixon and multi-echo T2*. There was no statistically significant difference between MRS and multi-echo T2* methods, and the Bland-Altman analysis found a mean difference of −0.54 ± 2.5% (95% CI −5.44%, 4.36%) between these two methods, indicating a strong agreement.

The primary source of the lack of agreement between the 2-point Dixon and other methods (MR spectroscopy and multi-echo T2*) is the consistent observation of elevated hepatic fat fraction values obtained from the 2-point Dixon compared to the other two techniques due to the inherent differences in the underlying principles and sensitivities of the imaging sequences.

Higher hepatic fat fraction values from the 2-point Dixon method were initially interpreted as an overestimation. This sequence, incorporating only 2 TE values, may not effectively account for variations in T2 relaxation times. This limitation can lead to inadequate correction for T2 relaxation effects on the signal, especially in tissues with varying fat compositions. Li et al's findings support this concern, highlighting that IP and OP images from the 2-point Dixon may inaccurately estimate hepatic fat content, especially when the liver fat content is lower than 5%.[28] Additionally, the study points out the intrinsic incorrectness of the fat fraction calculation based on IP and OP images due to the assumption that water and fat have a single resonance frequency, which is not valid for fat.

In contrast, MRS, with its acquisition of data at 5 different TEs, and multi-echo T2* sequence with 10 TEs, are designed to capture the complex T2 relaxation processes more comprehensively. The absence of sufficient T2 correction in the 2-point Dixon sequence may result in an overestimation of fat fraction, emphasizing the importance of understanding and addressing the potential limitations associated with the number of echo times employed in different imaging sequences. Kuhn et al's insights caution against potential biases in measurements, stating that accurate quantification of liver fat with chemical shift-encoded MRI, such as the 2-point Dixon, requires correction for T2* decay, T1 recovery, and spectral modelling of fat.[29] They highlight the necessity of correcting for confounding factors, particularly T2* decay, to avoid errors in calculating fat fraction. Kuhn et al's analysis recommends T2* correction for accurate fat quantification, contradicting assumptions that adequate correction necessitates using more than three echoes.

Despite these concerns, the convenience of the 2-point Dixon sequence being widely available on most MRI scanners makes it a pragmatic choice for routine clinical use Its strong correlation with both MRS and multi-echo T2* (correlation coefficients >0.9) suggests that it remains a reliable and clinically feasible option for many applications. However, its consistently higher hepatic fat fraction values compared to MRS and multi-echo T2* further underscore the importance of understanding its limitations. To ensure consistency in serial follow-ups and avoid misinterpreting method-dependent differences—such as Dixon's higher FF values—as true disease progression, patients should be monitored using the same imaging method throughout their follow-up examinations.

Interestingly, recent evidence by Qadri et al[30] provides an alternative interpretation. Their meta-analysis demonstrated that histological steatosis values often exceed MR-derived proton density fat fraction (PDFF), particularly at higher steatosis levels. While MR techniques quantify tissue triacylglycerol concentration, histology measures the fraction of lipid-containing hepatocytes, leading to discrepancies in results. Qadri et al reported that at higher levels of steatosis, histological measurements can exceed PDFF by up to 3.4-fold. This suggests that the higher values observed with the Dixon method may not represent overestimation but could align more closely with histological fat quantification.

Both explanations—overestimation due to insufficient T2 correction and alignment with histological scales—highlight the need for further research. Future studies should aim to resolve these discrepancies, validate MR methods against biopsy results, and establish conversion factors or thresholds that enable meaningful comparisons between imaging and histology-based fat quantification techniques.

The results of the correlation analysis among three fat fraction acquisition methods in different BMI and Waist Circumference Ratio groups show consistent findings. In patients with a normal BMI and those with a Waist Circumference Ratio below 100%, the group sizes were notably limited, comprising only 8 and 5 patients, respectively. As a result, Spearman correlation analysis was not conducted due to insufficient statistical power and the potential unreliability of correlation estimates from such small sample sizes.

In overweight and obese patients, robust and significant correlations were observed across all three fat fraction measurement techniques. The strongest correlations were found in the obese group, which suggests that the increased fat content in this population may enhance the sensitivity of the imaging methods.

Regarding WCR groups, all methods showed strong correlations, with the highest correlations seen in patients with a WCR between 120–140%. This suggests that central obesity, as reflected by WCR, may have a more pronounced effect on hepatic fat distribution and composition.

While higher fat content can indeed reduce RF penetration, the observed correlations in the obese group suggest that the increased hepatic fat still provided an adequate signal for these imaging methods. This may indicate that the methods are capable of capturing hepatic fat fractions effectively across a wide range of fat levels, despite potential limitations in RF penetration. Therefore, it is likely that the broader fat content range within the obese group contributed to the observed sensitivity of each method. Additionally, the larger variability in hepatic fat fraction values within the obese group may have contributed to the stronger correlations observed. The broader range of fat fraction values in this group likely increases the statistical relationship between methods, suggesting that the higher correlation coefficients may partly reflect the greater variability in hepatic fat content. This underscores the importance of considering variability when interpreting correlation strength across different body composition profiles.

Limitations

The sample size, especially in certain BMI and WCR groups, may affect the generalizability of the results. Additionally, the study's reliance on a single geographic location may limit the extrapolation of findings to diverse populations. Including participants undergoing bariatric surgery may introduce selection bias, and future studies should aim for more diverse and representative samples. We acknowledge that the differences in sampling volume across MRS, 2-point Dixon, and multi-echo T2* methods may introduce variability, as the overlap in tissue sampling cannot be precisely controlled and may be a source of measurement error. Lastly, the study's focus on specific hepatic fat assessment methods may exclude consideration of emerging technologies or alternative approaches.

Conclusion

In conclusion, this study highlights the robust correlations between MR spectroscopy, 2-point Dixon, and multi-echo T2* methods for assessing liver fat fraction, particularly in participants with higher BMI and WCR. These findings emphasize the importance of considering body composition profiles when interpreting and applying fat fraction measurement techniques.

For participants with suspected low hepatic fat content, Dixon and multi-echo T2* are preferable due to their ability to provide precise numerical fat fraction values, even in cases with minimal hepatic fat. MRS can still be a useful alternative when a numerical value is not required, particularly if the absence of a fat peak is deemed sufficient to exclude steatosis.

In cases of suspected high hepatic fat content, all three methods perform reliably. However, Dixon tends to provide systematically higher values compared to MRS and multi-echo T2*a consideration that should be factored into its use. Nonetheless, Dixon remains a strong option for stratifying high-fat participants or conducting population-level comparisons due to its robust correlation with the other methods.

For follow-up studies, maintaining consistency in the method used across assessments is critical to ensure reliable longitudinal comparisons. If a change in methodology is unavoidable, careful selection of alternative methods is necessary to minimize discrepancies, with multi-echo T2* and MRS serving as the most closely aligned substitutes. However, Dixon should be avoided as an alternative in follow-up settings where consistency with initial MRS or T2* measurements is required, due to its tendency to overestimate fat fraction values.

Abbreviations

BMI, Body Mass Index; BTFE, Balanced Turbo Field Echo; MRS, Magnetic Resonance Spectroscopy; MR, Magnetic Resonance; WCR, Waist Circumference Ratio; FF, Fat fraction; jMRUI, java-based Magnetic Resonance User Interface; ROI, Region of Interest; SPAIR, Spectral Adiabatic Inversion Recovery; SPSS, Statistical Package for Social Sciences; STEAM, Stimulated Echo Acquisition Mode; WHO, World Health Organization.

Funding

The study was financially supported by the Medical University of Gdansk, Poland (grant no. ST-111).

Disclosure

The authors report no conflicts of interest in this work.

References

1. World Health Organization. Obesity and overweight. 2021. Available: https://www.who.int/news-room/fact-sheets/detail/obesity-and-overweight. Accessed February 20, 2025.
2. Younossi ZM, Golabi P, Paik JM, Henry A, Van Dongen C, Henry L. The global epidemiology of nonalcoholic fatty liver disease (NAFLD) and nonalcoholic steatohepatitis (NASH): a systematic review. *Hepatology*. 2023;77(4):1335–1347. doi:10.1097/HEP.0000000000000004
3. Cornier MA, Dabelea D, Hernandez TL, et al. The metabolic syndrome. *Endocr Rev*. 2008;29:777–822. doi:10.1210/ER.2008-0024
4. Nilsson PM, Tuomilehto J, Rydén L. The metabolic syndrome – what is it and how should it be managed? *Eur J Prev Cardiol*. 2019;26:33–46. doi:10.1177/2047487319886404/ASSET/IMAGES/LARGE/10.1177_2047487319886404-FIG2.JPEG
5. Adams LA, Lymp JF, St. Sauver J, et al. The natural history of nonalcoholic fatty liver disease: a population-based cohort study. *Gastroenterology*. 2005;129:113–121. doi:10.1053/J.GASTRO.2005.04.014
6. Day CP, Anstee QM. Nonalcoholic fatty liver disease. *Semin Liver Dis*. 2015;35:203–206. doi:10.1055/S-0035-1562941
7. Camhi SM, Bray GA, Bouchard C, et al. The relationship of waist circumference and BMI to visceral, subcutaneous, and total body fat: sex and race differences. *Obesity*. 2011;19:402. doi:10.1038/OBY.2010.248
8. Semmler G, Balcar L, Wernly S, et al. Insulin resistance and central obesity determine hepatic steatosis and explain cardiovascular risk in steatotic liver disease. *Front Endocrinol*. 2023;14:1244405. doi:10.3389/FENDO.2023.1244405/BIBTEX
9. Ariya M, Koohpayeh F, Ghaemi A, et al. Assessment of the association between body composition and risk of non-alcoholic fatty liver. *PLoS One*. 2021;16:e0249223. doi:10.1371/JOURNAL.PONE.0249223
10. Wu Y, Li D, Vermund SH. Advantages and limitations of the body mass index (BMI) to assess adult obesity. *Int J Environ Res Public Heal*. 2024;21:Page757. doi:10.3390/IJERPH21060757
11. Lee ECZ, Anand VV, Razavi AC, et al. The global epidemic of metabolic fatty liver disease. *Curr Cardiol Rep*. 2024;26:199–210. doi:10.1007/S11886-024-02025-6/METRICS
12. Yin H, Fan Y, Yu J, et al. Quantitative US fat fraction for noninvasive assessment of hepatic steatosis in suspected metabolic-associated fatty liver disease. *Insights Imaging*. 2024;15:1–11. doi:10.1186/S13244-024-01728-2/FIGURES/3
13. Bohte AE, Van Werven JR, Bipat S, Stoker J. The diagnostic accuracy of US, CT, MRI and 1H-MRS for the evaluation of hepatic steatosis compared with liver biopsy: a meta-analysis. *Eur Radiol*. 2011;21:87. doi:10.1007/S00330-010-1905-5
14. Di Martino M, Bezzi M, Di Miscio R, et al. Comparison of magnetic resonance spectroscopy, proton density fat fraction and histological analysis in the quantification of liver steatosis in children and adolescents observational study. *World J Gastroenterol*. 2016;22:8812–8819. doi:10.3748/wjg.v22.i39.8812
15. Idilman IS, Keskin O, Celik A, et al. A comparison of liver fat content as determined by magnetic resonance imaging-proton density fat fraction and MRS versus liver histology in non-alcoholic fatty liver disease. *Acta Radiologica (Stockholm, Sweden: 1987)*. 2015;57:271–278. doi:10.1177/0284185115580488
16. Georgoff P, Thomasson D, Louie A, et al. Hydrogen-1 MR spectroscopy for measurement and diagnosis of hepatic steatosis. *AJR Am J Roentgenol*. 2012;199:2–7. doi:10.2214/AJR.11.7384
17. Pierre TG S, Clark PR, Chua-Anusorn W, et al. Noninvasive measurement and imaging of liver iron concentrations using proton magnetic resonance. *Blood*. 2005;105:855–861. doi:10.1182/BLOOD-2004-01-0177

18. Elfaal M, Supersad A, Ferguson C, et al. Two-point Dixon and six-point Dixon magnetic resonance techniques in the detection, quantification and grading of hepatic steatosis. *World J Radiol*. 2023;15:293–303. doi:10.4329/wjr.v15.i10.293
19. Grimm A, Meyer H, Nickel MD, et al. Evaluation of 2-point, 3-point, and 6-point Dixon magnetic resonance imaging with flexible echo timing for muscle fat quantification. *Eur J Radiol*. 2018;103:57–64. doi:10.1016/J.EJRAD.2018.04.011
20. Hutton C, Gyngell ML, Milanesi M, Bagur A, Brady M. Validation of a standardized MRI method for liver fat and T2* quantification. *PLoS One*. 2018;13:e0204175. doi:10.1371/JOURNAL.PONE.0204175
21. Orcel T, Chau HT, Turlin B, et al. Evaluation of proton density fat fraction (PDFF) obtained from a vendor-neutral MRI sequence and MRQuantif software. *Eur Radiol*. 2023;33:8999–9009. doi:10.1007/s00330-023-09798-4
22. Patil SB, Cannane S, Poyyamoli S, Anand RR, Kasi V. Role of advanced MRI techniques in the quantitative assessment of liver fat—a multimodality-based comparative study of diagnostic performance in a tertiary care institute. *J Gastrointest Abdom Radiol*. 2022;05:023–029. doi:10.1055/S-0041-1731964
23. Mouchti S, Orliacq J, Reeves G, Chen Z. Assessment of correlation between conventional anthropometric and imaging-derived measures of body fat composition: a systematic literature review and meta-analysis of observational studies. *BMC Med Imaging*. 2023;23:1–11. doi:10.1186/S12880-023-01063-W/FIGURES/3
24. Pienkowska J, Brzeska B, Kaszubowski M, Kozak O, Jankowska A, Szurowska E. MRI assessment of ectopic fat accumulation in pancreas, liver and skeletal muscle in patients with obesity, overweight and normal BMI in correlation with the presence of central obesity and metabolic syndrome. *Diabetes, Metab Syndr Obes Targets Ther*. 2019;12:623–636. doi:10.2147/DMSO.S194690
25. Pieńkowska J, Brzeska B, Kaszubowski M, Kozak O, Jankowska A, Szurowska E. The correlation between the MRI-evaluated ectopic fat accumulation and the incidence of diabetes mellitus and hypertension depends on body mass index and waist circumference ratio. *PLoS One*. 2020;15. doi:10.1371/JOURNAL.PONE.0226889
26. MRQuantif: MRI protocols. Available from: https://imagemed.univ-rennes1.fr/en/mrquantif/protocols. Accessed February 20, 2025.
27. Guiu B, Petit JM, Loffroy R, et al. Quantification of liver fat content: comparison of triple-echo chemical shift gradient-echo imaging and in vivo proton MR spectroscopy. *Radiology*. 2009;250:95–102. doi:10.1148/RADIOL.2493080217
28. Li Y-W, Jiao Y, Chen N, et al. How to select the quantitative magnetic resonance technique for subjects with fatty liver: a systematic review. *World J Clin Cases*. 2022;10:8906–8921. doi:10.12998/wjcc.v10.i25.8906
29. Kühn JP, Hernando D, Mensel B, et al. Quantitative chemical shift-encoded MRI is an accurate method to quantify hepatic steatosis. *J Magn Reson Imaging*. 2014;39:1494. doi:10.1002/JMRI.24289
30. Qadri S, Vartiainen E, Lahelma M, et al. Marked difference in liver fat measured by histology vs. magnetic resonance-proton density fat fraction: a meta-analysis. *JHEP Rep*. 2024;6:100928. doi:10.1016/J.JHEPR.2023.100928